Molecular BioSystems

Accepted Manuscript

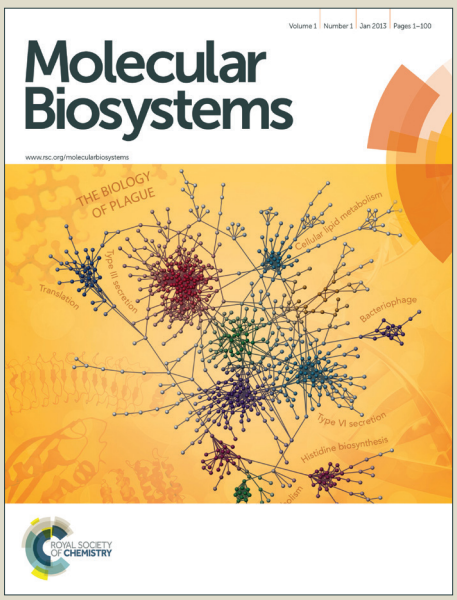

ROYAL SOCIETY OF CHEMISTRY

www.rsc.org/molecularbiosystems

Table of Content:

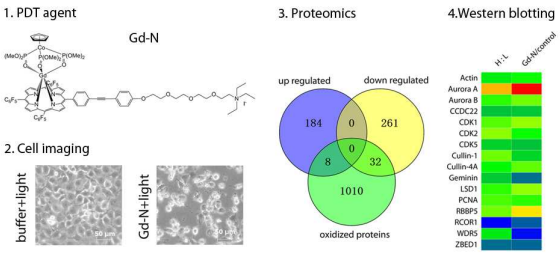

(8 cm x 3.8 cm)

A PDT agent Gd-N was successfully applied in SILAC based quantitative proteomics identifications of fast response targets to oxidative stress.

Molecular BioSystems

ARTICLE

SILAC-based Quantitative Proteomics Identified Lysosome as Fast Response Target to PDT agent Gd-N Induced Oxidative Stress in Human Ovarian Cancer IGROV1 cells

Received 00th January 20xx,
Accepted 00th January 20xx

DOI: 10.1039/x0xx00000x

www.rsc.org/

Dandan Qi, [a] Qianqian Wang, [a] Hongguang Li, [d] Tao Zhang, [d] Rongfeng Lan, [c*] Daniel W.J. Kwong, [d] Wai-Kwok Wong, [d] Ka-Leung Wong, [d*] Shuiming Li, [b*] and Fei Lu [a*]

Biological systems have developed an intact network and strategies in response to various environmental pressures such as irradiation, viral invasion and oxidative stress. Therefore, elucidation of the cellular response mechanism toward oxidative stress can contribute to the knowledge of redox regulation. By using newly developed gadolinium based photodynamic therapy (PDT) agent Gd-N and SILAC quantified proteomics analysis, we observed 485 proteins dysregulated in expression, 106 in phosphoprylation and 1050 in oxidation. Interestingly, lysosome was discovered as the main organelle affected by Gd-N induced singlet oxygen, along with the down regulation of a majority of lysosomal acid hydrolases and proton pump complex ATP6V/TCIRG1. Besides, phosphorylation sites with sequence patterns "TP" or "SP" were enriched in dysregulated phosphoproteins. Protein oxidization also exerts itself on sequence patterns in target proteins with "M.D" or "KM" taking methionine as the central residue. Oxidized proteins were most enriched in pathways of Parkinson's disease, an oxidative stress closely related neurodegenerative disease. In conclusion, our study reveals new insights on the cellular mechanism to oxidative stress and may contribute to the discovery of new targets and development of novel PDT agents.

Introduction

Oxidative stress raised by various elements is a universal phenomenon cells confronting during their lifespan. Cells evolutionally adapt a complete network or pathway to deal with the stress. But the mechanism regarding its regulation and signal transduction is still poorly understood. Closely related to redox regulation, photodynamic therapy (PDT) is a popularly used technology in clinical trials, which make use of artificially built agents and light induced reactive oxygen species (ROS) for medical treatment of acne or malignant cancers (1). ROS are chemically reactive molecules normally raised from the oxygen metabolism in cells. Upon environmental stress, ROS can increase dramatically and cause severe damage to the cell structures (2); hence, this feature can be used for cancer cell killing by introducing ROS specifically in a carcinoma focus (1). On the other hand, a cell is a

[a] Laboratory of Chemical Genomics, School of Chemical Biology & Biotechnology, Peking University Shenzhen Graduate School, Shenzhen 518055, China. lufei@pkusz.edu.cn [FL]
[b] Key Laboratory of Marine Bioresource and Ecology, College of Life Science, Shenzhen University, Shenzhen 518060, China. Shuimingli@szu.pku.cn [SML]
[c] Department of Chemistry, Hong Kong Baptist University, Kowloon Tong, Hong Kong. klwong@hkbu.edu.hk [KLW]
[d] Institute of Research and Continuing Education, Hong Kong Baptist University, Shenzhen 518057, China. rongfengl@hkbu.edu.hk [RFL]
[e] Ministry of Education Key Laboratory of Laser Life Science & Institute of Laser Life Science, College of Biophotonics, South China Normal University, Guangzhou 510631, China.

† Electronic Supplementary Information (ESI) available: [supplementary Figure S1-S4, and Tables S1-S6]. See DOI: 10.1039/x0xx00000x

complex and multimodal system in a highly dynamic microenvironment. PDT treatment remarkably enhances ROS in the cells and produced oxidization related proteins. Identification of the oxidative stress responding proteins and elucidation of their pathways may bring about a great advance in cellular redox regulation (3). In recent years, there is a growing need to develop cancer cells recognizing, in-depth light penetrating, and low dark cytotoxic PDT agents for reliable usages. We have previously developed a novel potential PDT agent, gadolinium porphyrinate (Gd-N), which had been designed and synthesized on the basis of Yb-N and shown high singlet oxygen quantum yield (51%) with characteristic near infrared (NIR) emission of the porphyrin upon photoexcitation (4, 5). Gd-N is capable of selectively targeting cancer cell through binding to anionic phospholipids of cell membrane and sufficiently killing cancer cells through light induced ROS. In addition, Gd-N is a nontoxic PDT agent and do not uptake by the normal cells, thus it is a biological friendly agent with the feature of near infrared (NIR) excitation and emission that can overcome the interference from autofluorescence and strong absorption in short wavelength of biological tissue. With this property, Gd-N can be applied in in-depth cancer specific imaging, in situ monitoring and NIR-induced photodynamic therapy.

Recently, the development of labelling approach has driven the mass spectrometry based proteomics to quantify and enabled the shotgun analysis of pooled samples from various processes, such as clinical serum or cell lysates for biological processes (6). Stable Isotope Labelling with Amino Acids in Cell Culture (SILAC) (7-9), as well as Isotope-Coded Affinity Tags (ICAT) (10) or Isobaric Tag for Relative and Absolute Quantitation (iTRAQ) (11) are now commonly used labelling techniques for quantitative proteomic analysis. This provides a method for identification of fast response genes or pathways of cells in response to extra or intra cellular stresses such as genomic disruption, interferon stimuli, and oxidative stress and so on.

On this basis, we would like to know how Gd-N induced ROS to impair the cell behaviour. In order to determine the proteins and their regulated networks involved in oxidative stress response, we performed SILAC based LC-MS/MS analysis in human ovarian cancer cell IGROV1, which is a cell line rich in protein expression. IGROV1 cells were incorporated with $^{13}C_6$ L-Lysine and $^{13}C_6$ $^{15}N_4$ L-Arginine for "Heavy" labelling to calculate the ratio of protein changes by taking the light amino acid labelled cells as the control upon mass spectrometry analysis. Interestingly, we found that lysosome was the major organelle responding to Gd-N induced oxidative stress, and 44 lysosomal proteins were obviously changed, especially the predominately down regulation of acid hydrolases. Besides, we also observed dysregulation of 44 mitochondria proteins; phosphorylation sites of 106 proteins, and also 1050 oxidized proteins. Among the oxidized proteins, they were highly enriched in Parkinson's disease and Huntington's disease, two classes of neurodegenerative disorders that closely related to oxidative stress. Moreover, SILAC based quantified proteins were confirmed by western blotting. In conclusion, this work will contribute to the understanding of cellular answering to sudden oxidative stress, especially in the situation of severe oxidative damage of lysosome by our Gd-N PDT agent, and also the recognition of protein oxidation regulation and related pathogenesis.

Materials and methods

Cell culture and stable isotope labelling

Human ovarian cancer cells IGROV1 were cultured in RPMI 1640 (GIBCO) medium supplemented with 10% fetal bovine serum as described previously (12). For incorporation of isotopic-labelled amino acid, two 3.5 cm dishes of 1×10^6 cells were respectively suspended with Heavy or Light SILAC media. SILAC media was prepared by Pierce SILAC Protein Quantitation Kits (Thermo Scientific, #89982) according to the manufacture's procedure. Briefly, a bottle of 450 mL SILAC RPMI 1640 medium was supplemented with 50 mL dialyzed fetal bovine serum and 50 mg $^{13}C_6$ L-Lysine-2HCl, 50 mg $^{13}C_6$ $^{15}N_4$ L-Arginine HCl for double labelling, marked as "Heavy". Similarly, another bottle of medium supplemented with L-Lysine-2HCl and L-Arginine-HCl was marked as "Light". Passage both cells for seven cell doublings by changing medium and splitting cells every two days to maintain cells are actively in log phase and achieve fully isotope incorporation.

Singlet oxygen treatment cells and Proteins SDS-PAGE

Heavy and Light isotope labelled cells were treated with light induced singlet oxygen generated by Gd-N, respectively, according to Zhang et al. (4). Briefly, Heavy isotope labelled cells were incubated with 2 μM Gd-N for 12 hours (Gd-N is a newly developed cancer cell selective-tracking gadolinium eradicator for photodynamic therapy, which exerts highly singlet oxygen yield but with no dark toxicity (4, 5)), and then irradiated with 0.5 J/m^2 generated from a 400-W

tungsten lamp fitted with a heat-isolation filter and a 500-nm long-pass filter under the fluency rate of milliwatts per square centimeter. After incubation for another 2 hours, cells were microscopic imaged, collected and lysed. Light isotope labelled cells was also treated as above but without adding Gd-N. Cell debris was removed by centrifugation at 14,000 rpm for 15 minutes. Determine protein concentration of each sample by BCA Protein Assay Kit and mix equal amounts of each cell lysate in a new tube. After adding SDS-PAGE loading buffer, samples were boiled for 10 minutes and centrifuged at 14,000 rpm for 5 minutes. Then, 250 μg total proteins were loaded onto one well of a gel and separated by SDS-PAGE using Hoefer SE400 Vertical Electrophoresis System (18×16 cm). Stain gel with coomassie brilliant blue G250 and excise total 27 protein bands continuously. Protein bands were destained in 50% (v/v) acetonitrile, dehydrated with gradient acetonitrile (50%-70%) and then Cysteine-alkylated by dithiothreitol/iodoacetamide. MS compatible peptides of each bands were generated by In-Gel trypsin digestion (Trypsin Gold, V5280, Mass Spectrometry Grade 100 μg (1 vial), Promega) at 37 ^{o}C for 16 hours and extracted using 70% acetonitrile (with 0.02% trifluoroacetic acid) for three times, combined the extracts and vacuum dried, resuspended in LC buffer (95% H_2O, 5% acetonitrile, 0.1% formic acid) and ready for Mass spectrometer analysis.

LC-MS/MS

Peptide fractions were injected under trapping conditions using an Eksigent nanoLC ultra 2D plus system. Trap and elute mode was used to separate each fraction using the microfluidics on a cHiPLC Nanoflex system equipped with a trap column (200 μm × 0.5 mm ChromXP C18-CL 3μm 120 Å) and a separation column (75 μm × 15 cm C18 3μm 120 Å). The gradient ran at 300 nL/min from 5% B (0.1% formic acid in acetonitrile) to 35% B over 120 min, rose to 85% B to wash the column, then re-equilibrated at 5% B for the next injection. Eluate was delivered into the mass spectrometer with a NanoSpray III source using a 10 μm i.d. nanospray tip (New Objective, Woburn, MA). Gas and other mass spectrometer settings used varied depending on optimization on each day, but typical values were curtain gas = 25, Gas 1 = 3−4, Gas 2 =0, an ion spray floating voltage around 2300, and a rolling collision energy voltage was used for CID fragmentation for MS/MS spectra acquisitions. Each cycle consisted of a TOF/MS spectrum acquisition for 250 ms (mass range 400−1250 Da), followed by acquisition of up to 50 MS/MS spectra (50 ms each, mass range 65−2000 Da) of MS peaks above intensity 150 taking 2.8 s total per full cycle. Once MS/MS fragment spectra were acquired for a particular mass, this mass was dynamically excluded for 25 s.

Data analysis

The AB SCIEX TripleTOF 5600 .wiff raw data were subjected to ProteinPilot 5.0 software (version 5.0.0.0, 4769) (with Paragon Algorithm 5.0.0.0, 4767) to generate peaks and build a result ".group project" file, for proteins identification and calculating peptides SILAC ratios (H:L) by searching against human uniprot-all.fasta database (Proteome ID=UP000005640, with reviewed protein count 20198). Parameters for identification: for MS1 initial mass error tolerance value =0.05 dalton and final mass error standard deviation value =0.0011 dalton, while for MS2, the initial mass error tolerance value=0.1 dalton and final mass error standard deviation value =0.01 dalton. Multi-precursor search function was used and 1 missed and/or non-specific cleavages were permitted. Phosphorylation@Ser, Thr, or Tyr, deamidation@Asn or Gln, oxidation@Met, Gln-> Pyro-Glu@ N-term, and acetyl-@protein N-terminus were set as variable modifications. Carboxymethyl@Cys was searched as a fixed modification. Bayesian protein confidence calculation was used for protein grouping. And peptide false discovery rate (FDR=1%) analysis was used to recalibrate peptide confidences. Auto bias correction of the quant results was used. Protein ratios were log2 transformed and the frequency distribution of the quantified proteins was calculated to determine differentially expressed proteins. All the raw data files for MS1 and MS2, the search results (including the detailed FDR summary for protein, distinct peptide and spectrum, the protein and distinct peptide summary, and the annotated and mass labelled spectra), search parameter files, as well as the reference search database have been deposited to the PeptideAtlas (http://www.peptideatlas.org) with the dataset identifier PASS00700 http://www.peptideatlas.org/PASS/PASS00700 (13).

Bioinformatics analysis

Proteins classification and Gene Ontology (GO) overrepresentative enrichment analysis were performed by PANTHER (Protein Analysis Through Evolutionary Relationships) (http://www.pantherdb.org) (14, 15), and PANTHER pathway and KOBAS were also used for pathway mapping (http://kobas.cbi.pku.edu.cn) (16, 17). Gene ID conversions were carried out using DAVID Bioinformatics Resources 6.7

(http://david.abcc.ncifcrf.gov) and bioDBnet (biological DataBase network, http://biodbnet.abcc.ncifcrf.gov) (18-20).

The protein-protein interactions network was established by STRING (Search Tool for the Retrieval of Interacting Genes/Proteins) database version 10.0 (21) and showed as evidence view. Figures were plotted by GraphPad Prism 5.0 (http://www.graphpad.com).

Phosphorylation sites and peptides sequences were subjected to motif-x (http://motif-x.med.harvard.edu) tool to extract the overrepresented patterns (22). Sequence width = 13, occurrences =15, significance = 0.000036 ($p<0.01$) and human protein database ipi.HUMAN.fasta were used. Oxidized sequence pattern searching was similarly performed and using "M" as central character. In addition, NetworKIN3.0 software tool (www.networkin.info) was used to map the kinases which responding for the phosphorylation of subjected sites (23). Heatmap was built by HemI 1.0 (Heatmap Illustrator, version 1.0) (http://www.biocuckoo.org) (24).

Western blotting

IGROV1 cells were subjected to Gd-N mediated PDT treatment (as described above) and harvested for western blotting of proteins, respectively. Briefly, collected cells were directly lysed in 1×sample buffer (62.5 mM Tris, pH=6.8, 2% SDS, 5% β-mercaptoethanol, 10% glycerol and 0.01% bromophenol blue) and boiled for SDS-PAGE separation. Western blotting was performed susing antibodies specific to proteins of interest. Antibodies were used as noted previously (25). Antibodies anti Aurora-A (#4718), was from Cell Signaling Technology. Inc. CCDC22 (#16636-1-AP), Actin (#60008-1-1g), were from Proteintech; CDC20 (#sc-8358), PCNA (#sc-56) were from Santa Cruz Biotechnology. Inc. WDR5 (#A302-430A), RBBP5 (#A300-931), RCOR1 (#A300-931) were from Bethyl Laboratories, Inc. Aurora B (#ab2254), LSD1 (#ab17721) were from abcam; and ZBED1 (#11040-5G1) from Sigma-Aldrich. Anti Geminin, Cullin-4A, CDK1, CDK2, CDK5, and Cullin-1 antibodies were laboratory made using purified antigen respectively (12, 26). Band intensity of western blotting results was analyzed through Gel Pro Analyzer software (Media Cybernetics, Inc. Rockville, MD20850, USA). Bands subjected to analysis were obtained from at least three independent experiments, the final average values were used to plot histogram.

Results

SILAC based quantitative proteomics identified proteins that respond to Gd-N induced oxidative stress in IGROV1 cells.

We have newly developed a two photon activated photodynamic therapy agent Gd-N, which binds specifically to cancer cell membrane to realize cancer-target therapy (4). It is also a near infrared radiation induced PDT agent, and exerts no dark toxicity to living cells. Although we have proved binding to anion phospholipids (phosphatidylserine and phosphatidylcholine) facilitate the specific targeting of Gd-N to cancer cells but not normal cells, it is still unclear how Gd-N induced reactive oxygen species can sufficiently kill cancer cells and how cancer cells response to oxidative stress (Figure 1 and references (4)). Herein, we performed SILAC based quantitative proteomics analysis, through labelling Lysine and Arginine with heavy isotope amino acids (as "Heavy"), and comparing with the normal amino acid cultured cells (as "Light") to identify the fast response cellular proteins or organelles (Figure 1A, B and C). A total of 6649 proteins were identified using the criteria described in the Experimental Procedures at a false discovery rate (FDR) of 1%, and among them, 92.30% (5681/6155) were quantified. Totally 535129 spectra for 136447 peptides were obtained with a cutoff of (unused >0.05) (Figure 1D), and 83.68% (4754/5681) of the quantified proteins contain at least two unique peptides (Figure 1E and F). Among the 4754 quantified proteins, we successfully sorted out 485 dysregulated proteins (10.20%, 485/4754), in which 60.41% (293/485) of them were down regulated along with other 192 proteins of up regulated (Figure 1F, Table S1). Detailed searching parameters for protein identification and quantification, classified proteins list are available in supporting information Table S1 and the PeptideAtlas (http://www.peptideatlas.org) (refer to Experimental Procedures).

Lysosome was identified as the major organelle affected by oxidative stress.

It is interesting to figure out the functions and cellular components of the 485 dysregulated proteins that obviously respond to oxidative stress. For this purpose, we performed PANTHER protein overrepresented enrichment analysis to classify the above proteins. We found that both up regulated and down regulated proteins belong to 9 classes of molecular functions, in which proteins classified to catalytic activity or binding shared most portions of the proteins (about 75% of 485) (Figure 2 A and B, Table S2). We also sorted the proteins according to their cellular components, and

interestingly discovered that membrane bound organelle proteins were most enriched (Figure S1, A and B, Table S2). These results suggested that intracellular membrane bound organelles like lysosome, mitochondrion, or Golgi apparatus and endoplasmic reticulum may be deeply affected by Gd-N mediated PDT treatment.

In addition, we also try to figure out which biological pathways the dysregulated proteins participated in

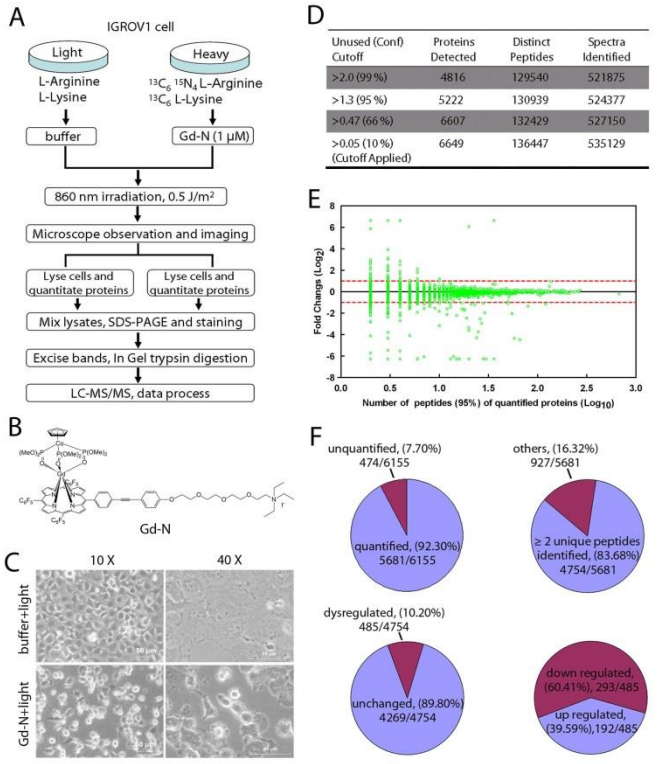

Figure 1. SILAC based identification and quantification of responsive targets to Gd-N induced oxidative stress. (A) Workflow of cell culture, experimental treatment and quantitative proteomics analysis. Gd-N is a newly developed cancer cell selective photodynamic therapy reagent in our previous work. (B) Chemical structure of Gd-N. (C) Microscopic imaging of IGROV1 cells phenotypes changes upon near infrared light (860 nm) activated Gd-N ROS releasing. (D) Summary of mass spectrometry analysis results. (E) Scatter plot of proteins relative changes (quantified by H: L) in contrast to the abundance of their identified peptides. The red dash lines indicate a 2.0-fold cutoff. (F) Pie charts present the general results for proteins quantification.

response to oxidative stress. The 485 dysregulated proteins were subjected to multi-database integrated annotation tool KOBAS 2.0 for pathway analysis. And consistently, we found that lysosome pathways are those with most hits (Figure 2C, Table S2 and S3). Moreover, metabolic pathways like Glycan degradation, Glycosphingolipid and lipoprotein metabolism, as well as binding and uptake of ligands by scavenger receptors pathways were also enriched (Figure 2C).

Furthermore, the 485 dysregulated proteins were subjected to searching against STRING analysis for protein-protein interactions to figure out whether the proteins interact with each other directly or through intermediate molecules. Surprisingly, both the up regulated and down regulated proteins were closely

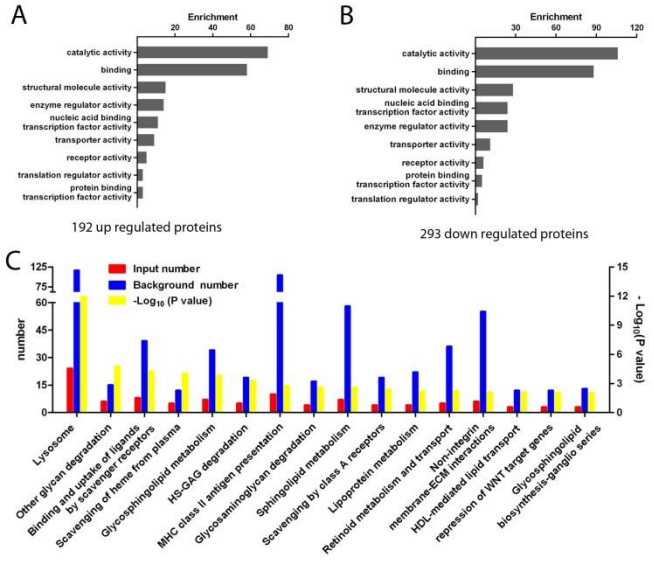

Figure 2. PANTHER Gene Ontology (GO) overrepresented enrichment analysis of the 485 dysregulated proteins. The Molecular Functions classifications of (A) 192 upregulated, and (B) 293 down regulated proteins. (C) KOBAS pathway analysis of total 485 dysregulated proteins. Lysosome was identified as the major organelle to be affected.

interacted and yielded rich interactions nodes in the general view (Figure S2, A and B). For the up regulated proteins, cell cycle and transcriptional regulatory proteins, as well as oxidative stress responding proteins were multiply connected (Figure S2, A) (the circular contains CDC20, AURKA, CHEK1, CDKN1A et al for cell cycle proteins, DNAH8, MEN1, SMARCC1, TERF1, SMAD1 for transcriptional regulations). In contrast, for the down regulated proteins, lysosomal proteins especially the acidic hydrolases exerted tight interactions (Figure S2, B, the circular with purple and white colored proteins, the cathepsins family (CTS), HEXA/B etc.). Besides, lipoproteins like APOE, APOA1, APOB etc. and histone modification proteins formed another two hot interaction sites. These results indicate that cells introduced multi-dimensional strategies like metabolic pathways and signal transductions to deal with the emergency oxidative stress. As a lipophilic PDT agent, Gd-N is highly enriched

in membrane bound organelle like lysosome that is responsible for detoxification; thus it is heavily impaired.

In order to clearly display the process of lysosomal proteins in response to oxidative stress, we prepared a graph taking KEGG lysosome pathway as the chief source to show the changed proteins (Figure 3). Lysosome formation proteins (VPS18, CHMP3, CHMP1A, STAM, MSRB2) and intralysosomal acid hydrolases (including cathapsins, CTS family, HEXA/B, or GAA etc.)

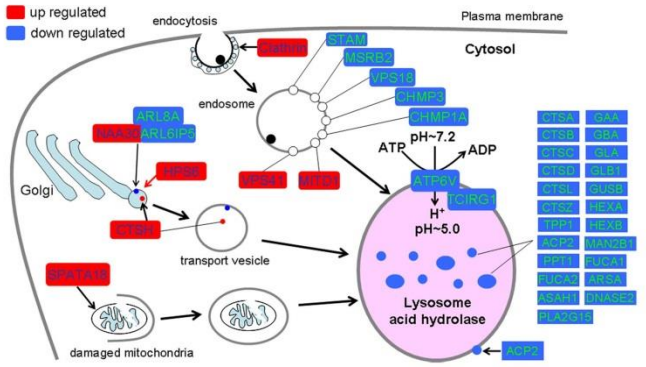

Figure 3. Cartoon model elucidated the lysosome centered response to Gd-N induced reactive oxygen species in human ovarian cancer IGROV1 cells. Both up (red) and down (blue) regulated lysosomal proteins were presented.

were down regulated. Interestingly, the proton pump ATP6V/TCIRG1 localized in lysosomal membrane that is responsible for maintaining the acid pH of intra lysosome lumen was seriously down regulated. It was possible that severe oxidative stress destroyed the integrity of lysosome membrane, thus in order to avoid collateral damage to peripheral cell structures by the out flowed acid hydrolases, cells need to shut down the proton pump, that facilitates the deactivation of hydrolases in the weak alkaline environment.

Protein phosphorylations were wildly regulated in response to oxidative stress.

With the elucidation of proteins that participated in oxidative stress response, we would like to know the effect of known protein modifications like phosphorylation, oxidation. Firstly, we picked up a list of phosphorylated peptides, which contains all the phosphorylated peptides and their proteins, including sites, sequences, and also the quantified H:L ratio (Figure 4A and Table S4). Among them, we identified 346 unique phospho-sites with the cutoff of 95% (confidence), and 85.55% (296/346) of them was quantified (Figure 4A). Moreover, 35.81% (106/296) of the quantified phosphorylated sites were dysregulated, and 16.04% (17/106) of them were up regulated in contrast with the 83.96% (89/106) down regulated sites (Figure 4A and B). In addition, most of the phosphorylation sites (80.19%, 85/106) were regulated at phosphorylation level only (Figure 4A, bottom right panel). Annotated and mass labelled spectrum for all the phosphopetides were deposited on the PeptideAtlas (identifier PASS00700). Secondly, we want to know if there are sequence similarities or patterns within the quantified dysregulated phosphor-peptides. Phosphopeptides

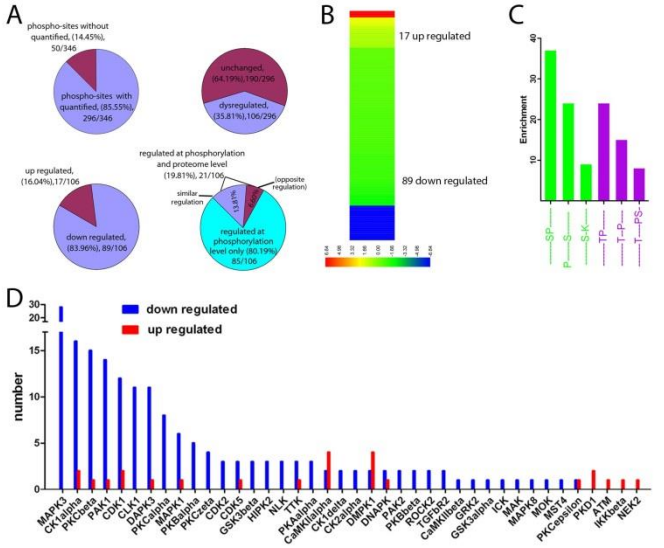

Figure 4. Identifications of phosphorylated peptides in Gd-N mediated PDT treated samples. (A) Pie charts showed 346 unique phosphorylated sites, in which 85.55% (296/346) of them were quantified. 35.81% (106/296) of the quantified phosphorylated sites were dysregulated, while 16.04% (17/106) of them were upregulated in contrast with the 83.96% down regulated sites. In addition, most of the phosphorylation sites (80.19%, 85/106) were regulated at phosphorylation level only. (B) Heatmap showed the general view of the alterations of dysregulated phosphor-proteins. (C) Six conserved sequence pattern were identified by motif-x tool (http://motif-x.med.harvard.edu). (D) NetworKIN software tool (www.networkin.info) was used to map the potential kinases that responding for the phosphorylation of 106 dysregulated sites.

along with their site information were subjected to motif-x tool to extract the overrepresented patterns. Six conversed sequence patterns were mapped (Figure 4C and Figure S3A). They mostly belonged to “SP” or “TP” pattern. Then it is interesting to explore the potential kinases that are in charge of phosphorylating. Many databases and software have been established for this prediction. Here we selected the literature based NetworKIN 3.0 software tool to predict the most

likely kinases which are responding for the phosphorylation of the 106 dysregulated sites. We found that total 40 kinases were predicted for the dysregulated protein phosphorylations (Figure 4D, and Tablse S5). For down regulated phosphorylation sites, MAPK3, CK1alpha, PKCbeta, PAK1, CDK1, CLK1 and DAPK3 are the top seven kinases that all have over 10 sites. MAPK3 is a kinase activated by upstream signal, leading to its translocation to the nucleus where it phosphorylates substrates. Inhibition of MAPK3 was observed in oxidative stress induced apoptosis (27). Consistently, we found down regulated phosphorylation sites were mostly related to the substrates of MAPK3. But the situation changed in up regulated phosphorylation sites, CaMKIIalpha, DMPK1, CK1alpha, PKD1 and ATM are the top five kinases with the most hits (Figure 4D). CaMKIIalpha is the Ca^{2+} calmodulin kinase II that responds to changes of cellular redox state and can be activated by oxidative stress (28, 29). The up regulation of protein phosphorylation we found in CaMKIIalpha substrates was in line with the activation of this kinase upon Gd-N induced oxidative stress. These results may suggest that different regulations for up and down regulated phosphorylation sites, or different pathways may be involved in response to oxidative stress.

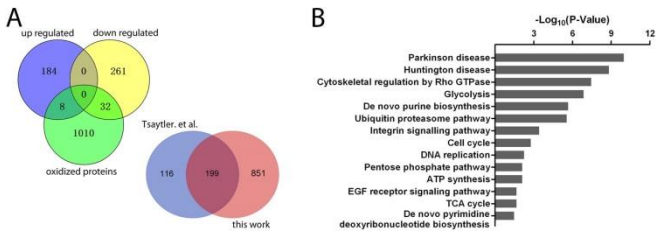

Figure 5. Identifications and classifications of the oxidized proteins. (A) Venn diagram showed the overlap relationship among up regulated, down regulated and oxidized proteins. Consistently, 63.17% (199/315) of the oxidized proteins were overlapped with the results of Pavel A. Tsaytler et al. (B) PANTHER pathways analysis. Parkinson's disease was discovered to be the most enriched pathway.

In addition, we also evaluated the protein interactions among the proteins with phosphorylation changes (Figure S3, B). Surprisingly, DNA topoisomerase TOP2A served as the major node for proteins with phospho-modification changes, while other transcriptional regulators like SRRM1, SRRM2, etc. were connected. We also noted that proteins participating in oxidative stress response like BAG6, TPR etc. were also closely interacted; these proteins were also the important factors in Parkinson's disease pathway, a pathway mainly happens in neuron tissues and shared similar factors for oxidative stress regulation.

Protein oxidations in response to ROS stress.

Protein oxidations wildly happen in photodynamic therapy treatment (PDT). PA.Tsaytler. et al. firstly performed proteomic identifications of fast response targets to ROS and they discovered 315 oxidized proteins (3). Protein oxidation is related to the subcellular localizations of PDT agents and mostly in the form of thiol oxidation (30). On this basis, we focused on the methionine oxidation upon Gd-N induced ROS stress. We identified 1050 oxidized proteins which belong to 37 biological processes according to PANTHER GO-Slim classification, the metabolic process especially the protein metabolism

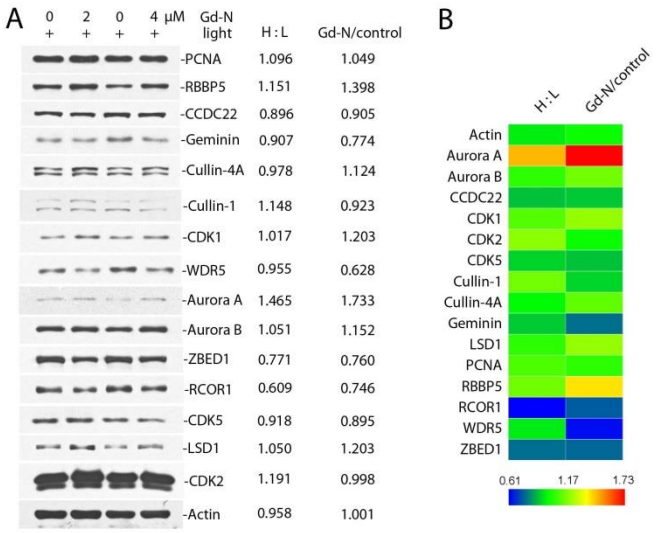

Figure 6. Representative western blotting showed the changes of protein expression. (A) Interested proteins were detected using antibodies as indicated, respectively. Relative protein bands intensity was measured by Gel-Pro Analyzer (version 4.0.00.001) and calculated the ratio of Gd-N treatment to control. Three replications were used. (B) Heatmap showed the comparisons of western blotting results with SILAC quantified data.

was the most abundant process (Figure S4, A and Table S6).In the classification by molecular functions, catalytic activity and oxidoreductase activity were also among the top enriched classes (Figure S4, B). These results were consistent with the changes of proteins as mentioned above (in Figure 2A and B). In addition, ribonucleoprotein complex was the most enriched class according to the GO-Slim cellular component analysis (Figure S4, C). The most interesting result we discovered is that the 1050 oxidized proteins exerted top enrichment in Parkinson's disease and Huntington's disease (Figure 5, B). This inspired us to explore the

relationship between Parkinson's disease pathway and our discovered oxidized proteins. Parkinson's disease is a central nervous system degenerative disorder and mainly affects the motor system. It results from the death of dopamine-generating cells in the substantia nigra of midbrain, but the reason for this cell death is poorly understood (31). It is proposed that proteosomal and lysosomal system dysfunction and reduced mitochondrial activity may cause cell death (32). In this work, we found that 40 proteins related to Parkinson's disease were oxidized. In light of the very similar cellular model of oxidative stress between Parkinson's disease and PDT treatment, it is possible to identify the targets for Parkinson's disease research and potential therapy strategy, or even elucidate the mechanism of the disease pathogenesis.

Furthermore, we compared the 1050 oxidized proteins with the 485 dysregulated proteins, the results in venn diagram showed that oxidized proteins can also change in expression level, and more likely to be down regulated (Figure 5A, up left panel), for 10.92% (32/293) of the down regulated proteins were oxidized, in contrast to 4.17% (8/192) up regulated proteins. In addition, our data consistently shared the oxidized proteins with the pioneer results of PA. Tsaytler. et al. (3), because the two groups of data shared 199 proteins, and we covered 63.17% (199/315) of proteins from PA. Tsaytler. et al.'s work (Figure 5A, downright panel). Considering the different treatment to introduce cellular oxidative stress, these results suggested that the cell possesses a complete but similar regulatory network to respond to oxidative stress caused by various extra- or intra-cellular factors. Moreover, we were interested in exploring the sequence patterns of oxidized proteins. All 1050 oxidized proteins were subjected to motif-X analysis (10, 22). Surprisingly, three sequence patterns were mapped. They are ".....M.D....", ".....KM....." and "D.....M....." (Significance factor=0.000036, $p<0.01$) (Figure S4, D). These results suggested that protein oxidizations also have conserved motifs to be recognized and modified, similar to the situation of phosphorylation.

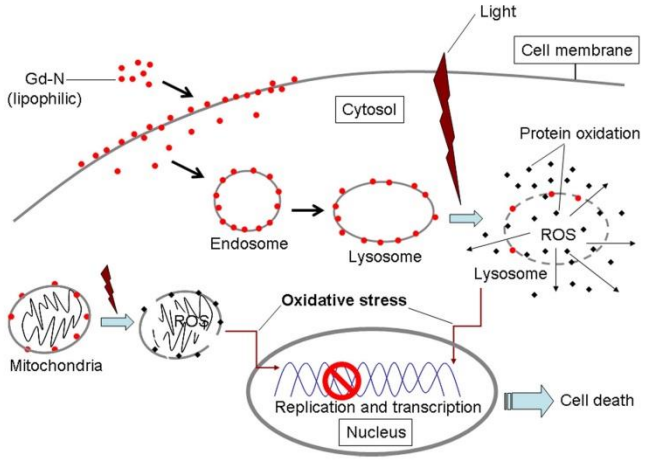

Figure 7. Schematic diagram elucidates the proposed answering mechanism to Gd-N induced singlet oxygen. Lipophilic Gd-N can bind to cancer cell membrane and intracellular localized through endocytosis or partially penetrated and absorbed by mitochondria. Upon light excitation, Gd-N produced a sudden increase of singlet oxygen and made oxidative stress, lysosome was the main organelles been heavily affected. Serious oxidative damage to cell structures and proteins triggered redox response, along with protein level changes, and modification alterations. Furthermore, severe oxidative stress can deeply impair cell proliferation, DNA replication and transcription, and even induce cell death.

Protein changes observed by western blotting were in line with the results of SILAC based quantification.

In order to confirm the protein changes quantified by SILAC based proteomics, we performed western blotting analysis to detect protein alterations in the same sample for SILAC experiments. Proteins bands were measured by Gel-Pro Analyzer and the ratio between Gd-N treatment and control sample was calculated. Average ratio of three experiments was obtained (Figure 6A). Then a heatmap was generated by using HemI 1.0 software to view the ratio data from both SILAC and western blotting experiments (24). In addition, the two sets of data showed a Poisson correlation coefficient of 0.7959. The above results indicate the SILAC based quantification of proteomics is reliable (Figure 6B).

Lysosome was severe affected in Gd-N induced cellular oxidative stress.

Oxidative stress is a common event in cell lifespan. Severe oxidative stress will quickly lead to cell death especially in cancer cells, and this feature can be used for cancer specific targeting and therapy. We identified and quantified over 6000 proteins using SILAC based strategy and obtained rich information about cell response to sudden oxidative stress introduced by newly explored photodynamic therapy agent Gd-N, a newly PDT agent which can specific bind to cancer membrane. We found that lysosome is severely affected in response to oxidative stress induced by this type of PDT agent, and proteins phosphorylation and oxidation were closely related to the regulation of oxidative stress. We proposed an interesting cartoon diagram that lysosome is seriously affected by Gd-N

induced reactive oxidative species, because Gd-N can enrich in lysosome through specific binding to cell membrane and endocytosis process (Figure 7). The serious damage to lysosome or even mitochondria caused singlet oxygen exerted severe oxidative stress on cell survival. In this situation, cell will adapt effective measures like shut down the lysosomal proton pump, destroy of acid hydrolase to avoid secondary damage to cellular structures. Besides, signal raised by oxidative stress can rapidly transduce into nucleus to regulate DNA replication and transcription, likely through phosphorylation of key factors.

Discussion

Reactive oxygen species (ROS) are consistently produced and eliminated in living cells, which are closely related to cell proliferation and death, and even the pathological situations like inflammation, carcinogenesis and metastasis (33). Elevating or reducing ROS can be used as strategy for cancer therapy (34). Normally, photodynamic therapy takes use of exogenous but light controllable ROS production agent to realize clinical application. Many kinds of PDT agents have been designed and synthesized for the potential uses of different purposes, while most of them are aimed at cancer therapy. We have previously developed a novel gadolinium based PDT agent Gd-N, which can sufficiently produce ROS to kill cancer cell (4). Then we used Gd-N as a model molecule to make oxidative stress in IGROV1 cells that labelled with isotopic amino acids for quantitative proteomic analysis. We discovered that lysosome was the most affected organelle along with down regulation of a majority of acid hydrolases as well as proton pump ATP6V/TCIRG1 complex localized on lysosomal membrane. Lysosome is an important organelle for cell homeostasis of removing misfolded proteins or damaged organelles. From the above results, we can propose that when serious damage came to lysosome, cells will take two strategies to eliminate the damage, a) shut down and down regulation of proton pump to relieve the acidic environment of lysosomal lumen, b) degradation of lysosomal hydrolases. Both of the two methods are aimed at avoiding the destructive activities of hydrolases to other cell structures. Besides, we also observed dysregulated phosphorylation of 106 proteins and 1050 oxidized proteins. Through kinase substrate mapping and conserved sequence pattern analysis, we found MAPK3 and CaMKIIalpha are the kinases respectively in charge of down or up regulation of proteins upon oxidative stress. Furthermore, intrinsic pathway and regulation pattern for cellular oxidative stress may be adopted to answering instant ROS crisis like PDT treatment, or age related unsatisfied clearance of oxidative stress in neuron tissues, for example the Parkinson's disease. Given that we surprisingly discovered that the ROS induced oxidized proteins were most enriched in Parkinson's disease related pathway, we hope these results can be useful hints for both future neurodegenerative diseases research and PDT agent development.

Conclusions

In this work, we used our recently explored gadolinium porphyrinate (Gd-N) as a two photon induced photodynamic therapy agent to identify the fast response targets in ovarian cancer IGROV1 cells. Using SILAC based quantitative proteomics and bioinformatics analysis; we successfully identified a majority of lysosomal acid hydrolases and proton pump complex ATP6V/TCIRG1 as obviously affected proteins in lysosome. Conserved sequence patterns "TP" or "SP" were enriched in dysregulated phosphoproteins and "M.D" or "KM" taking methionine as the central were identified in oxidized proteins. Consistently, oxidized proteins were most enriched in oxidative stress related pathways or even clinical lesions like Parkinson's disease. Thus, a clear and whole proteome work on cellular oxidative stress response is useful for the identification of novel PDT targets and design of next generation of PDT agents.

Acknowledgements

This work was supported by the grants from National Natural Science Foundation of China (NSFC) (21402167, 21133002), Natural Science Foundation of Guangdong Province (2014A030313779) and from The Hong Kong Research Grants Council (HKBU 203013), Hong Kong Baptist University (FRG1/14-15/015).

References

1. Dougherty, T. J., Gomer, C. J., Henderson, B. W., Jori, G., Kessel, D., Korbelik, M., Moan, J., and Peng, Q. (1998) Photodynamic therapy. *J Natl Cancer Inst.* 90, 889-905.
2. Stadtman, E. R. (1992) Protein oxidation and aging. *Science.* 257, 1220-1224.
3. Tsaytler, P. A., M, C. O. F., Sakharov, D. V., Krijgsveld, J., and Egmond, M. R. (2008) Immediate protein targets of

photodynamic treatment in carcinoma cells. *J Proteome Res.* 7, 3868-3878.
4. Zhang, T., Lan, R., Chan, C. F., Law, G. L., Wong, W. K., and Wong, K. L. (2014) In vivo selective cancer-tracking gadolinium eradicator as new-generation photodynamic therapy agent. *Proc Natl Acad Sci U S A.* 111, E5492-5497.
5. Zhang, T., Chan, C. F., Lan, R., Li, H., Mak, N. K., Wong, W. K., and Wong, K. L. (2013) Porphyrin-based ytterbium complexes targeting anionic phospholipid membranes as selective biomarkers for cancer cell imaging. *Chem Commun (Camb).* 49, 7252-7254.
6. Bijian, K., Mlynarek, A. M., Balys, R. L., Jie, S., Xu, Y., Hier, M. P., Black, M. J., Di Falco, M. R., LaBoissiere, S., and Alaoui-Jamali, M. A. (2009) Serum proteomic approach for the identification of serum biomarkers contributed by oral squamous cell carcinoma and host tissue microenvironment. *J Proteome Res.* 8, 2173-2185.
7. Geiger, T., Cox, J., Ostasiewicz, P., Wisniewski, J. R., and Mann, M. (2010) Super-SILAC mix for quantitative proteomics of human tumor tissue. *Nat Methods.* 7, 383-385.
8. Ong, S. E., Blagoev, B., Kratchmarova, I., Kristensen, D. B., Steen, H., Pandey, A., and Mann, M. (2002) Stable isotope labeling by amino acids in cell culture, SILAC, as a simple and accurate approach to expression proteomics. *Mol Cell Proteomics.* 1, 376-386.
9. Zheng, P., Xiong, Q., Wu, Y., Chen, Y., Chen, Z., Fleming, J., Gao, D., Bi, L., and Ge, F. (2015) Quantitative proteomics analysis reveals novel insights into mechanisms of action of long noncoding RNA HOTAIR in HeLa cells. *Mol Cell Proteomics.* 14(6), 1447-1463.
10. Gygi, S. P., Rist, B., Gerber, S. A., Turecek, F., Gelb, M. H., and Aebersold, R. (1999) Quantitative analysis of complex protein mixtures using isotope-coded affinity tags. *Nat Biotechnol.* 17, 994-999.
11. Ross, P. L., Huang, Y. N., Marchese, J. N., Williamson, B., Parker, K., Hattan, S., Khainovski, N., Pillai, S., Dey, S., Daniels, S., Purkayastha, S., Juhasz, P., Martin, S., Bartlet-Jones, M., He, F., Jacobson, A., and Pappin, D. J. (2004) Multiplexed protein quantitation in Saccharomyces cerevisiae using amine-reactive isobaric tagging reagents. *Mol Cell Proteomics.* 3, 1154-1169.
12. Yin, F., Lan, R., Zhang, X., Zhu, L., Chen, F., Xu, Z., Liu, Y., Ye, T., Sun, H., Lu, F., and Zhang, H. (2014) LSD1 regulates pluripotency of embryonic stem/carcinoma cells through histone deacetylase 1-mediated deacetylation of histone H4 at lysine 16. *Mol Cell Biol.* 34, 158-179.
13. Desiere, F., Deutsch, E. W., King, N. L., Nesvizhskii, A. I., Mallick, P., Eng, J., Chen, S., Eddes, J., Loevenich, S. N., and Aebersold, R. (2006) The PeptideAtlas project. *Nucleic Acids Res.* 34, D655-658.
14. Mi, H., Muruganujan, A., Casagrande, J. T., and Thomas, P. D. (2013) Large-scale gene function analysis with the PANTHER classification system. *Nat Protoc.* 8, 1551-1566.
15. Mi, H., Muruganujan, A., and Thomas, P. D. (2012) PANTHER in 2013: modeling the evolution of gene function, and other gene attributes, in the context of phylogenetic trees. *Nucleic Acids Res.* 41, D377-386.
16. Nikolsky, Y., and Bryant, J. (2009) Protein networks and pathway analysis. Preface. *Methods Mol Biol.* 563, v-vii.
17. Xie, C., Mao, X., Huang, J., Ding, Y., Wu, J., Dong, S., Kong, L., Gao, G., Li, C. Y., and Wei, L. (2011) KOBAS 2.0: a web server for annotation and identification of enriched pathways and diseases. *Nucleic Acids Res.* 39, W316-322.
18. Huang da, W., Sherman, B. T., and Lempicki, R. A. (2009) Systematic and integrative analysis of large gene lists using DAVID bioinformatics resources. *Nat Protoc.* 4, 44-57.
19. Huang da, W., Sherman, B. T., and Lempicki, R. A. (2009) Bioinformatics enrichment tools: paths toward the comprehensive functional analysis of large gene lists. *Nucleic Acids Res.* 37, 1-13.
20. Mudunuri, U., Che, A., Yi, M., and Stephens, R. M. (2009) bioDBnet: the biological database network. *Bioinformatics.* 25, 555-556.
21. Szklarczyk, D., Franceschini, A., Wyder, S., Forslund, K., Heller, D., Huerta-Cepas, J., Simonovic, M., Roth, A., Santos, A., Tsafou, K. P., Kuhn, M., Bork, P., Jensen, L. J., and von Mering, C. (2014) STRING v10: protein-protein interaction networks, integrated over the tree of life. *Nucleic Acids Res.* 43, D447-452.
22. Schwartz, D., and Gygi, S. P. (2005) An iterative statistical approach to the identification of protein phosphorylation motifs from large-scale data sets. *Nat Biotechnol.* 23, 1391-1398.
23. Horn, H., Schoof, E. M., Kim, J., Robin, X., Miller, M. L., Diella, F., Palma, A., Cesareni, G., Jensen, L. J., and Linding, R. (2014) KinomeXplorer: an integrated platform for kinome biology studies. *Nat Methods.* 11, 603-604.
24. Deng, W., Wang, Y., Liu, Z., Cheng, H., and Xue, Y. (2014) HemI: a toolkit for illustrating heatmaps. *PLoS One.* 9(11). e111988.
25. Lan, R., Lin, G., Yin, F., Xu, J., Zhang, X., Wang, J., Wang, Y., Gong, J., Ding, Y. H., Yang, Z., Lu, F., and Zhang, H. (2012) Dissecting the phenotypes of Plk1 inhibition in cancer cells using novel kinase inhibitory chemical CBB2001. *Lab Invest.* 92, 1503-1514.
26. Wang, J., Lu, F., Ren, Q., Sun, H., Xu, Z., Lan, R., Liu, Y., Ward, D., Quan, J., Ye, T., and Zhang, H. (2011) Novel histone demethylase LSD1 inhibitors selectively target cancer cells with pluripotent stem cell properties. *Cancer Res.* 71, 7238-7249.
27. Scioli, M. G., Cervelli, V., Arcuri, G., Gentile, P., Doldo, E., Bielli, A., Bonanno, E., and Orlandi, A. (2014) High insulin-induced down-regulation of Erk-1/IGF-1R/FGFR-1 signaling is required for oxidative stress-mediated apoptosis of adipose-derived stem cells. J Cell Physiol. 229, 2077-2087.
28. Bouallegue, A., Pandey, N. R., and Srivastava, A. K. (2009) CaMKII knockdown attenuates H2O2-induced phosphorylation of ERK1/2, PKB/Akt, and IGF-1R in vascular smooth muscle cells. Free Radic Biol Med. 47, 858-866.
29. Nogueira, N. P., de Souza, C. F., Saraiva, F. M., Sultano, P. E., Dalmau, S. R., Bruno, R. E., Goncalves Rde, L., Laranja, G.

A., Leal, L. H., Coelho, M. G., Masuda, C. A., Oliveira, M. F., and Paes, M. C. (2011) Heme-induced ROS in Trypanosoma cruzi activates CaMKII-like that triggers epimastigote proliferation. One helpful effect of ROS. PLoS One. 6, e25935.
30. Yuan, K., Liu, Y., Chen, H. N., Zhang, L., Lan, J., Gao, W., Dou, Q., Nice, E. C., and Huang, C. (2014) Thiol-based redox proteomics in cancer research. Proteomics. 15, 287-299.
31. Shulman, J. M., De Jager, P. L., and Feany, M. B. (2011) Parkinson's disease: genetics and pathogenesis. Annu Rev Pathol. 6, 193-222.
32. Obeso, J. A., Rodriguez-Oroz, M. C., Goetz, C. G., Marin, C., Kordower, J. H., Rodriguez, M., Hirsch, E. C., Farrer, M., Schapira, A. H., and Halliday, G. (2010) Missing pieces in the Parkinson's disease puzzle. Nat Med. 16, 653-661.
33. Schumacker, P. T. (2006) Reactive oxygen species in cancer cells: live by the sword, die by the sword. Cancer Cell. 10, 175-176.
34. Martindale, J. L., and Holbrook, N. J. (2002) Cellular response to oxidative stress: signaling for suicide and survival. J Cell Physiol. 192, 1-15.